

# Phase Shift Technique for the Measurement of Chromatic Dispersion in Optical Fibers Using LED's

BRUNO COSTA, DANIELE MAZZONI, MARIO PULEO, AND EMILIO VEZZONI

**Abstract**—A sinusoidal technique is reported, which allows simple and accurate measurements of chromatic dispersion in optical fibers. It is based on the phase shift which a sinusoidally modulated light beam undergoes while traveling along a fiber when its wavelength is changed. The choice of a multiple LED's source permits the continuous spectral covering from 750 to 1600 nm; easily available instrumentation and devices are needed for the measurement setup.

The technique is reported in detail by showing results obtained in multimode fibers; statistical evaluation of its accuracy and a comparison with conventional methods are carried out.

An accuracy of a few picoseconds in relative delay and of  $\pm 1$  ps/nm · km in chromatic dispersion are demonstrated, that compare very favorably with the existing techniques.

## INTRODUCTION

**A**N intrinsic limit to the information carrying capacity of optical fibers is set by the wavelength dependence of the propagation constant, resulting in chromatic dispersion and in consequent bandwidth penalty. Hence, the need of an efficient measurement technique to evaluate chromatic dispersion properties of optical fibers in an accurate and possibly simple way is felt.

Most of the measurements reported up to now make use of pulse techniques, in which the time delays between pulses of different wavelengths after traversing a known length of fiber are measured; hence, the chromatic dispersion, resulting from material and waveguide dispersion, defined as  $d\tau/d\lambda$  ( $\tau$  = time delay per unit length of fiber,  $\lambda$  = wavelength) can be calculated. The need of a satisfactory time resolution, mainly around the wavelength of zero chromatic dispersion (ZCD), where very small relative delays are to be measured, calls for the use of fast laser sources. To obtain the necessary wide spectral coverage, either several lasers at different wavelengths [1], [2], or nonlinear effects in crystals [3] or fibers [4] pumped by high power pulsed lasers have been used.

Such experimental setups, although supplying high level optical output pulses which allow a large dynamic margin, are cumbersome and very expensive. In addition, temporal and wavelength resolution are limited by the width of the pulses, typically a few hundreds of picoseconds; furthermore, the widely used Raman systems (employing a Nd-Yag laser and a single-mode fiber) suffer from jitter and optical triggering instabilities, which may be difficult to reduce by additional arrangements to within limits acceptable in the ZCD region.

This paper describes the first transmission measurement of chromatic dispersion with a much simpler and highly accurate sinusoidal technique over the wavelength range 750–1350 nm, thus covering the so-called first and second window slightly above the ZCD wavelength. The full range extension up to 1500 nm can be easily performed. The first report on the successful operation of this technique over a wide spectral range can be found in [5], while a suggestion on this line had already been given by Ozeki and Watanabe [6] although, as far as we know, no subsequent development was carried out.

The basis of the present technique lies in using broad spectrum and comparatively inexpensive LED sources, and modulating them sinusoidally; the relative phase shifts between different wavelengths, progressively selected by means of a monochromator after traversing the fiber under test, allow the evaluation of chromatic dispersion.

Using such a method we could obtain both the highly accurate determination of chromatic delay, and hence dispersion, on a wide spectral range, and the precise and repeatable determination of the wavelength of ZCD.

In this paper the results obtained by this technique are compared with those obtained by conventional methods.

An experimental statistical evaluation of the accuracy in the ZCD wavelength determination is carried out. Finally, the excellent time and wavelength resolution provided by the method have allowed us to observe fine features in the delay curve, and, in particular, to point out an anomalous behavior in correspondence to OH absorption peaks.

## EXPERIMENTAL SETUP

Fig. 1 shows the experimental setup. The source is an LED that is changed according to the spectral region under investigation, in front of which a fiber pigtail is mounted; the fiber being tested is connected to the pigtail by a demountable splice (Springgroove®<sup>1</sup> [7]) and, at the opposite end, is coupled to a monochromator by means of an optical system that matches the numerical apertures. The light from the monochromator is similarly coupled to the detector, that is, a silicon long wavelength improved APD up to 1.1  $\mu$ m, and a germanium APD for longer wavelengths. A low noise transimpedance amplifier follows the detector.

The LED is sinusoidally modulated at 32 MHz by a signal

Manuscript received March 15, 1982; revised June 23, 1982.

The authors are with CSELT, Torino, Italy.

<sup>1</sup>Patent pending.

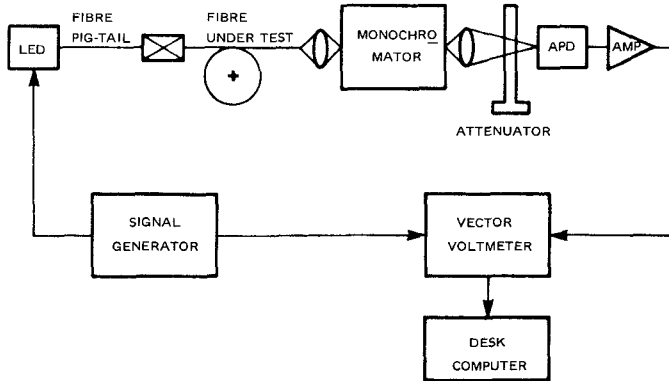


Fig. 1. Schematic of the experimental setup.

generator with good stability characteristics. The modulation frequency is chosen as the highest allowed by the bandwidths of the LED's to achieve the best temporal resolution.

As the signal travels along the fiber, its phase changes, also on account of the wavelength dependence of group velocity, according to

$$\varphi(\lambda) = 2\pi f_0 \tau_g(\lambda) = 2\pi f_0 L/v_g(\lambda) \quad (1)$$

where  $f_0$  is the modulation frequency,  $L$  is the fiber length,  $v_g(\lambda)$  is the wavelength-dependent group velocity of the signal, and  $\tau(\lambda)$  is the corresponding group delay. Phase differences among different wavelengths are measured by a vector voltmeter, with a resolution of 0.1 degrees, which corresponds to about 8 ps at the working frequency. This is the major intrinsic limitation to time resolution, the uncertainty due to the signal generator instability. Yet, the actual precision limit to the relative delays (or phase shifts) measurement is set by the presence of noise. Hence, the maximum uncertainty of the measured delays can be estimated in a round figure of  $\pm 10$  ps for  $S/N$  ratios better than 30 dB (electrical).

In order to get rid of any wavelength-dependent phase shift other than that due to the fiber (mainly the chromatic delay of LED's), the system is calibrated by measuring the phase changes, having placed the fiber pigtail in front of the monochromator.

If the calibration is carried out after the measurement, an optical variable attenuator at the output of the monochromator can be adjusted to exactly compensate for the fiber attenuation; in this way the optical level impinging on the APD is the same at a given wavelength, both during calibration and measurement, thus virtually removing any possible error due to the undesired influence of the signal amplitude on the phase along the receiving chain (detector-amplifier-vector voltmeter).

A desk-top computer is used to collect data and to perform calculations.

## RESULTS AND DISCUSSIONS

The method and the measurement system have been tested first on a low attenuation, standard telecommunication graded index fiber, manufactured by Corning Glass (4 dB/km maximum attenuation over the range of interest, 62  $\mu\text{m}$  core size, 0.2 NA, 1.1 km long).

Four surface emitting LED's from different manufacturers have been used in order to cover the widest possible wave-

length range, their central wavelengths being, respectively, 0.83 (Northern Telecom), 0.9 (SGS/ATES), 1.06 (Varian), and 1.27  $\mu\text{m}$  (Plessey). Fig. 2 shows the electrical  $S/N$  ratios at the receiver for each LED after the pigtail. The shape results mainly from the LED's spectra and from the spectral response of the detectors; the 30 dB sensitivity gap between the peak at 1.3  $\mu\text{m}$  and the three lower wavelength peaks are due to the higher noise contribution of the germanium APD, in comparison with the silicon one. To improve the  $S/N$  ratio, a bandpass electrical filter with a bandwidth of 1 MHz has been placed at the vector voltmeter input. The horizontal line, corresponding to a  $S/N$  ratio of 30 dB, is the limit under which the phase becomes too unstable to keep measurements within the desired precision limits.

The calibration curves of the apparatus (mainly due to the chromatic delay of the sources) are shown in Fig. 3 for each LED. Let us notice that, due to their order of magnitude (several hundreds of picoseconds), they must be taken into account anyway.

The delays are taken at 5 nm intervals, and the monochromator exit slit is set to give a 5 nm linewidth; this seems to be a good tradeoff between high resolution and high  $S/N$  ratios.

Fig. 4 shows the result for each of the four ranges, already free from calibration delays. As expected, the delay decreases while increasing wavelength, until it finds a minimum slightly above 1.3  $\mu\text{m}$ . All the experimental points look very regularly arranged as a result of the good  $S/N$  ratio, even at the two ends of each range, corresponding to the extreme emission tails of the LED.

To find out easy-to-handle equations tightly fitting the experimental points, we made use of a conventional technique [8]; as the modulating waveform propagates along the fiber with group velocity  $v_g(\omega) = (d\beta(\omega)/d\omega)^{-1}$ ,  $\beta(\omega)$  being the propagation constant, the group delay can be expressed by

$$\tau_g(\omega) = L \frac{d\beta(\omega)}{d\omega} \quad (2)$$

from which the chromatic delay can be evaluated. The calculations become simpler assuming a plane wave propagating along the fiber and neglecting waveguide effects. These conditions seem sensible although in a narrow range around the ZCD wavelength material and wavelength dispersion become comparable. With the further assumption that the relative energy contents of different modes keep constant with wavelength, both in amplitude and relative delay (as it is commonly assumed in the literature), the chromatic delay becomes

$$\tau_g(\lambda) = \frac{L}{C} \left[ n(\lambda) - \lambda \frac{dn}{d\lambda} \right]. \quad (3)$$

Being  $n(\lambda)$  precisely expressed by the well-known Sellmeier equation,  $\tau_g(\lambda)$  can be obtained differentiating that function according to (3). To avoid the outcoming awkward form, we can resort to the following simpler series expansions of the form:

$$\tau_g(\lambda) = A + B\lambda^{-2} + C\lambda^2 \quad (4)$$

or

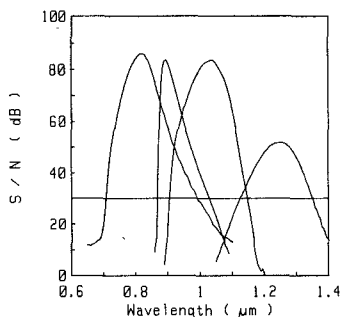


Fig. 2. Electrical  $S/N$  ratios at the receiver for each LED, after the pigtail. The 30 dB continuous horizontal line is the limit for accepting experimental data.

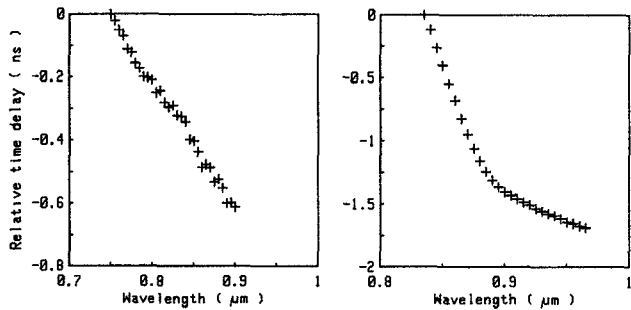


Fig. 3. Chromatic delay calibration for the four LED's.

$$\tau_g(\lambda) = A + B\lambda^{-2} + C\lambda^2 + D\lambda^{-4} + E\lambda^4. \quad (5)$$

The shorter one can be used with satisfactory precision over almost the whole range, while the higher order one is needed in the fourth range, around the ZCD wavelength. The continuous traces in Fig. 4 joining the experimental points were obtained by this procedure.

The simple derivative of (4) or (5), according to the choice, results in the required chromatic dispersion curves of the fibers, as shown in Fig. 5. These results demonstrate that it is possible, with only four LED sources, to perform a high resolution measurement of chromatic dispersion over a 600 nm wide spectral range, from 0.75-1.35  $\mu\text{m}$ . At the same time, the ZCD wavelength can be calculated, as can be seen from the fourth insert of Fig. 5.

To obtain the overall delay curve from the four subranges, a simple procedure is used, which allows a more precise matching of two adjacent regions.

This procedure consists of extending the fitting curve calculated in one range to the center wavelength of the next one and conversely, in order to establish the relative posi-

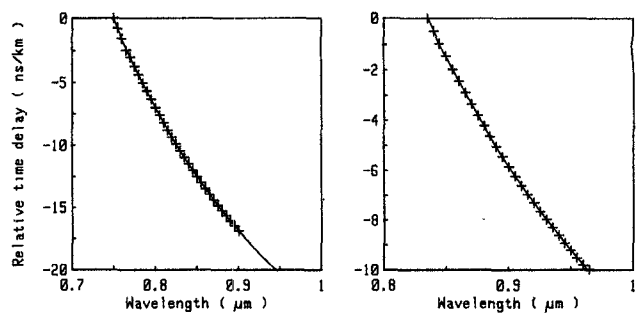


Fig. 4. Measured time delays with fitting curve, free from calibration delays, for a Ge doped borosilicate optical fiber.

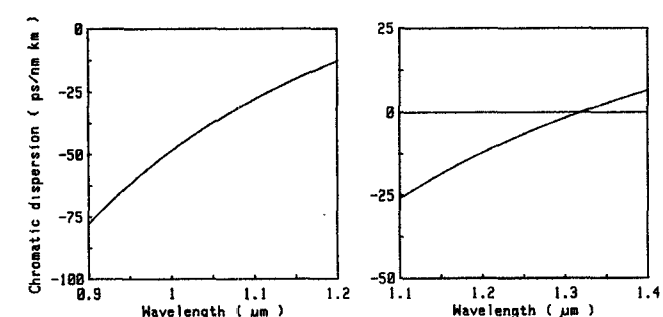
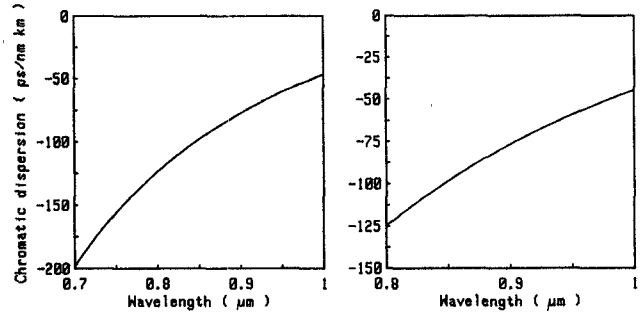


Fig. 5. Calculated chromatic dispersion curves, as obtained by derivation of the fitting curves from Fig. 4.

tioning as exactly as possible. Once all the experimental points (delays) are joined, a new overall fitting equation can be calculated (Fig. 6).

The method is useful to avoid that the simple linking of the experimental points in the overlapping regions where the  $S/N$  ratio is poorer, introduces inaccuracies; furthermore, it is essential when two adjacent regions show no common points (with acceptable  $S/N$  ratio) at all, as can be seen to happen between 1.10 and 1.15  $\mu\text{m}$ .

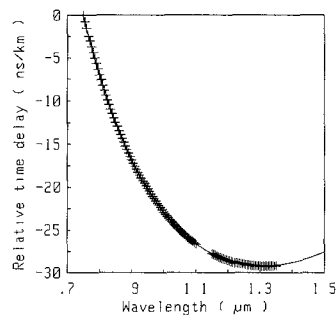


Fig. 6. Time delay in the whole spectral range, as obtained by the jointing procedure.

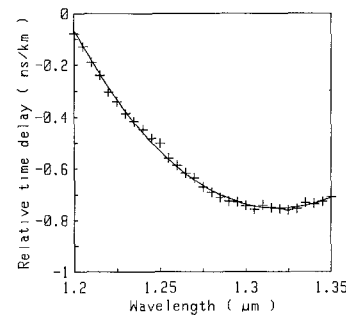


Fig. 8. Expanded view of Fig. 5 in the 1.3  $\mu\text{m}$  range; notice the non-smooth behavior around 1.3  $\mu\text{m}$  and the small bump at 1.24  $\mu\text{m}$ .

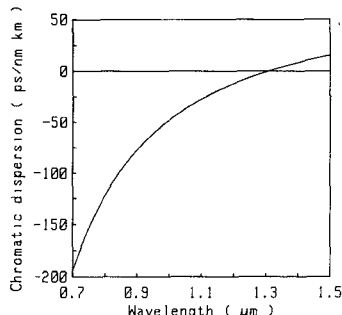


Fig. 7. Calculated chromatic dispersion from Fig. 6.

Fig. 7 shows the corresponding full-range material dispersion, obtained by differentiation of the overall delay curve. The low slope of the dispersion curve around the zero axis crossover (about 1 ps/nm  $\cdot$  km per 10 nm) results in a high sensitivity of the determination of the ZCD wavelength to measurement errors.

Fig. 8 shows an expanded view of the delay curve around 1.3  $\mu\text{m}$ . A couple of qualitative remarks can be made. Near the minimum, a nonsmooth, saddle-like behavior is apparent, while at 1.24  $\mu\text{m}$  a small bump is recognizable, corresponding to a weak (less than 1 dB/km) hydroxyl absorption peak in the spectral attenuation of the fiber. Although these details are almost of the same order of magnitude as noise, in a region where each relative delay results from the difference between near equal quantities, yet they were observed in a number of measurements.

To test the repeatability of the determination of the ZCD wavelength, 14 independent measurements were made, each one with its own calibration, in the 1.15–1.35  $\mu\text{m}$  region. An expanded view of the results is shown in Fig. 9, where it can clearly be seen that all the curves have nearly the same slope, and that they are very regularly distributed in a small wavelength range. The results of this repeatability test are summarized in the histogram of Fig. 10, which shows a mean value of 1303 nm and a standard deviation of less than 1 nm. This allows us to conclude that this method is intrinsically repeatable within  $\pm 1$  nm.

This intrinsic repeatability is strictly connected to the optical launching conditions, which were kept constant throughout the repeatability test. Indeed, the excitation of different mode distributions could result in considerable ZCD wavelength differences; as shown in [9], differences of even 15–20 nm can be found between the ZCD wavelengths typical of selectively excited groups of modes. This is confirmed, as

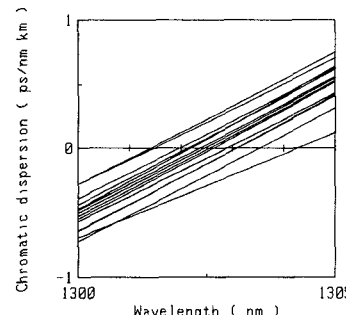


Fig. 9. Expanded view of the zero crossover from 14 independent dispersion measurements carried out on the same fiber to test the repeatability of the method.

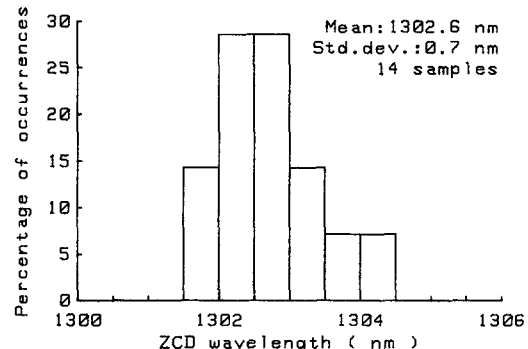


Fig. 10. Histogram of ZCD wavelengths as resulting from the repeatability test.

well, by a comparison between the dispersion curves of Fig. 5, fourth insert, and Fig. 9, which were both obtained from the same fiber, but in different launching conditions. In the first situation, a lensed fiber pigtail was used in front of the LED to increase coupling efficiency, and the ZCD wavelength was found to be about 1315 nm; in the second condition, a simpler butt coupling was accepted, resulting in a ZCD wavelength of 1303 nm.

These variations result from the contributions of both waveguide dispersion, which depends on the mode number, and from the dispersive properties of the core material that depend, in general, on the dopant level and are therefore different at different radial coordinates; considering that each mode is distributed over a different core region, it is clear that the chromatic dispersion is, in general, mode dependent, and in particular, the ZCD wavelength is dependent on the excitation conditions.

Let us notice that, when used to determine the ZCD wavelength, the high order fitting curve calculated in the single

1.3  $\mu\text{m}$  range gives the most accurate results, fitting the experimental points better than the overall fitting curve.

From the same repeatability test over 14 independent measurements, it can be ascertained that the maximum uncertainty on the evaluated dispersion is  $\pm 1 \text{ ps/nm} \cdot \text{km}$  (peak-to-peak) for any wavelength in the spectral region 1.15–1.35  $\mu\text{m}$ , and  $\pm 0.3 \text{ ps/nm} \cdot \text{km}$  (peak-to-peak) at 1.3  $\mu\text{m}$ , which is consistent with the uncertainty of  $\pm 1 \text{ nm}$  (standard deviation) on the determination of the ZMD wavelength, being the slope of the curve at 1.3  $\mu\text{m}$  about 1  $\text{ps/nm} \cdot \text{km}$  per 10 nm.

Typical deviations between the measured delays and the corresponding fitting curve, always from 1.15 to 1.35  $\mu\text{m}$ , are of the order of 6 ps rms thus confirming the *a priori* estimated figures, and evidencing that the system is close to the resolution limits of the vector voltmeter ( $\pm 0.1$  degree, corresponding to  $\pm 8 \text{ ps}$ , at the frequency of 32 MHz). A possible way to overcome this instrumental limitation would consist in using sources permitting higher modulation bandwidths, for instance edge emitting LED's.

Repeatability figures similar, or even better, to those given in the 1.3  $\mu\text{m}$  range can be confirmed in the low wavelength ranges (1.06, 0.9, and 0.82  $\mu\text{m}$ ), where advantage can be taken of the superior Si APD noise figure.

A recent publication [10] reports a time resolution of 10 ps, obtained using a plurality of injection lasers with picosecond pulses; this result approaches the one we have shown.

To conclude the discussion of the system relative accuracy, let us notice that a possible source of errors are the midterm thermal drifts of the LED chromatic delay, which should be kept within acceptable limits during both calibration and measurement. Fig. 11 shows a typical variation of the calibration curve of a 1.3  $\mu\text{m}$  LED emitter due to a thermal gradient of 10°C, resulting in a maximum deviation of about 150 ps. Therefore, to avoid inaccuracies, the source temperature should be kept stable within  $\pm 0.5^\circ\text{C}$ , which is a sensible demand.

To test the absolute accuracy of the present method, a comparison was made against dispersion measurements performed on the same fiber with the widely used pulse technique, employing a Raman-laser facility.

This reference system, described elsewhere [11], consists of a Nd-Yag laser, operating at 1.064  $\mu\text{m}$ , both *Q*-switched and mode locked; its output pulses pump a single-mode fiber, where single pass stimulated Raman scattering takes place, with a spectrum extending up to 1.85  $\mu\text{m}$ . A purposely developed synchronizing setup keeps the total electrical jitter within  $\pm 25 \text{ ps}$  (peak-to-peak). The relative delays between pulses at different wavelengths are taken from the sampling scope and processed with averaging and fitting procedures. The relative time delays measured at the output of a graded index optical fiber (62  $\mu\text{m}$  core size, 0.2 NA, 1080 m long) with very low attenuation, supplied by Corning Glass, are reported in Fig. 12, together with the delay data obtained with the sinusoidal technique. As can be seen, the agreement is excellent. By derivation of the Sellmeier-type fitting equation, the chromatic dispersion can be calculated, as obtained with the two different techniques. As shown in Fig. 13, the two curves almost overlap, with a maximum difference lower than 2  $\text{ps/nm} \cdot \text{km}$ , at the edges. The ZCD wavelength results to be, respectively, 1301 and 1304 nm, with a difference of 3 nm. (To reduce

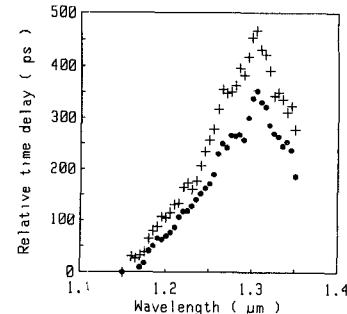


Fig. 11. Dependence of the 1.3  $\mu\text{m}$  LED calibration curve on temperature (dots:  $T = 25^\circ\text{C}$ ; crosses:  $T = 15^\circ\text{C}$ ).

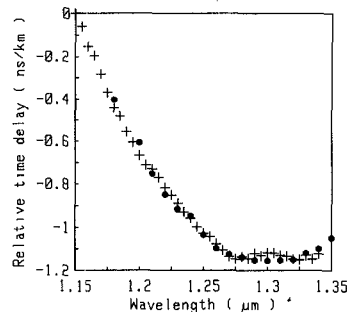


Fig. 12. Comparison between the relative time delay as measured with the LED/sinusoidal technique (crosses) and as measured with the Raman laser/pulse technique (dots).

possible variations due to different launching conditions, the single-mode Raman generating fiber is coupled to the fiber under test through a 1 m long step index fiber, working as a mode mixer; the LED sources, on the other hand, make use of long fiber pigtails, to strip out possible cladding modes.)

The good results of the comparing test allow us to conclude that no significant systematic error affects the measurements. Furthermore, the sinusoidal technique (6 ps stability) seems to be less sensitive than the pulsed one to jitter troubles and midterm instabilities (up to about  $\pm 50 \text{ ps}$ ) which adversely affect the Nd-Yag system; this is confirmed by inspection of Fig. 12. On the other hand, the last one has much more dynamic reserve, due to the high level of the output pulses.

Finally, while the LED sinusoidal technique can be easily extended from 750 to 1600 nm, the Raman laser pulsed system seems less adaptable, requiring either a double span technique with a frequency doubler, or a very efficient ultra-low loss single-mode fiber capable of generating useful levels of anti-Stokes lines below 1.064  $\mu\text{m}$ .

The sinusoidal technique requires the use of a few broad spectrum sources to cover a wide spectral range. This implies the need of exploiting the extreme tails of the LED's spectrum, where the optical power is low and the *S/N* ratio at the receiver consequently decreases. With the nonselected devices at our disposal, assuming a minimum acceptable *S/N* ratio of 30 dB, the dynamic margin of the system, as measured at the input of the vector voltmeter, can be obtained from Fig. 2. For instance, a dynamic margin of more than 30 dB can be attained in the range 0.75–1.1  $\mu\text{m}$ , corresponding to a fiber attenuation of 15 dB: more than enough to test most of the commonly used fibers. In the 1.3  $\mu\text{m}$  region the margin is lower, mainly due to the poor performance of the Ge APD. Yet, with the use of selected highly efficient emitters, some improvement in coupling efficiency, the further reduction of the electrical

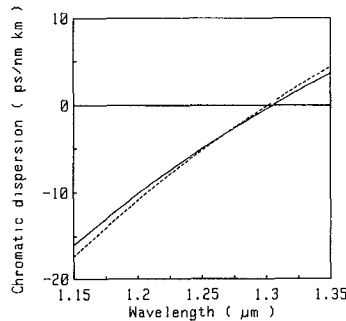


Fig. 13. Comparison between the chromatic dispersion curves obtained from the data of Fig. 12. The continuous line refers to the sinusoidal technique (ZCD at 1304 nm), the dashed line refers to the pulse technique (ZCD at 1301 nm).

filter bandwidth, and a careful selection of the central wavelengths (e.g., 1.1, 1.2, 1.3, 1.4, 1.5  $\mu\text{m}$ ), should enhance the performances of the system in the long wavelength region; there it seems reasonable to reach a dynamic margin not too far from 20 dB (10 dB optical), a satisfactory target in a region where the fiber attenuation is actually very low.

A clear demonstration of the technique's effectiveness due to its high resolution and accuracy, is found when studying dispersion anomalies. For testing purposes, measurements were made on a high OH content fiber, with a peak attenuation of several tens of dB at 940 nm, and a lower peak of 18 dB at 880 nm. The sinusoidal technique evidences the presence of a relevant anomalous delay increase around 880 nm, thus confirming the similar, but less evident, observation made on a different fiber at 1240 nm. Between 925 and 1000 nm, the measurement is impractical, due to the high attenuation.

As the simple Sellmeier-derived series expansions (4) and (5) fail in a correspondence of anomalies, we preferred to make use of a spline fitting procedure, whose derivative gives the dispersion curve reported in Fig. 14 (continuous line). A dramatic swing can be seen around 880 nm, corresponding to the peak in the attenuation curve (dotted line). The dashed curve is the Sellmeier-type fit, obtained eliminating the anomalous points. (It is worthwhile noticing the excellent matching between the two adjacent ranges 0.8–0.9  $\mu\text{m}$  and 1.0–1.1  $\mu\text{m}$ , across a wide region (100 nm) lacking experimental data, around the 940 nm peak, that was carried out by the above-mentioned jointing technique.)

Regarding the interpretation of such anomalies, further investigations carried out at our laboratory [11] have shown that they could be explained either in terms of differential mode attenuation or as an intrinsic effect of the material. In any case, they should be taken into account for an accurate determination of chromatic dispersion values, particularly of the ZCD wavelength.

## CONCLUSIONS

We have reported in detail a novel sinusoidal technique for chromatic dispersion measurements in optical fibers over an extended wavelength range, which exhibits very high accuracy and makes use of simple and easily available instrumentation and components. Extensive testing was performed that evidenced high precision both in full range dispersion determination and ZCD wavelength definition. Absolute precision was

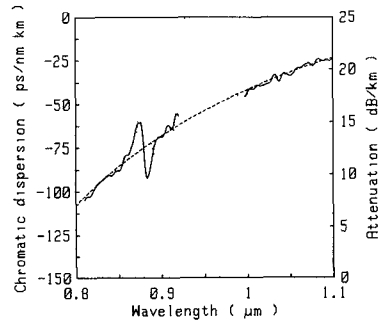


Fig. 14. Dispersion curve of a high OH content fiber, as obtained from a spline curve fitting the experimental data (continuous line) and as obtained, excluding the anomalous points around 880 nm, from an expanded Sellmeier-type fitting equation (dashed line). The anomalous swing is clearly shown, corresponding to the 880 nm peak of the spectral attenuation (dotted line).

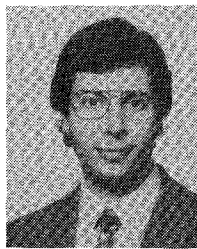
tested too, by comparison with a well-established pulse technique, resulting in excellent agreement.

The system's effectiveness was demonstrated as well by the accurate resolution of dispersion anomalies due to OH absorption.

The extension to the whole range of interest, 0.75–1.6  $\mu\text{m}$ , can be easily performed, while some improvement is surely possible to increase sensitivity in the 1.1–1.6  $\mu\text{m}$  region. In this way the extension of measurements to monomode fibers should be feasible, and we are currently investigating this problem. In particular, the use of edge emitting diodes should provide coupled powers to monomode fibers completely adequate for the measurement.

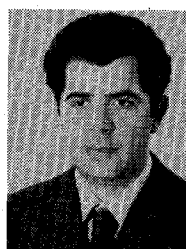
## REFERENCES

- [1] D. Gloge, E. L. Chinnock, and T. P. Lee, "Ga As twin-laser set up to measure mode and material dispersion in optical fibres," *Appl. Opt.*, vol. 13, no. 2, pp. 261–263.
- [2] B. Sordo, F. Esposto, and B. Costa, "Experimental study of modal and material dispersion in spliced optical fibres," in *Proc. 4th European Conf. on Opt. Commun.*, Genova, Italy, Sept. 12–15, 1978, pp. 71–79.
- [3] D. N. Payne and A. H. Hartog, "Determination of the wavelength of zero material dispersion in optical fibres by pulse-delay measurements," *Electron. Lett.*, vol. 13, no. 21, pp. 627–629.
- [4] L. G. Cohen and C. Lin, "Pulse delay measurements in the zero material dispersion wavelength region for optical fibres," *Appl. Opt.*, vol. 16, no. 12, pp. 3136–3139.
- [5] B. Costa, D. Mazzoni, M. Puleo, and E. Vezzoni, "Highly accurate and simple technique for material dispersion measurements in optical fibres," in *Proc. 7th European Conf. Opt. Commun.*, Copenhagen, Denmark, Sept. 8–11, 1981, p. 5.3.
- [6] O. Takeshi and A. Watanabe, "Measurements of wavelength dependence of group delay in a multimode silica fibre," *Appl. Phys. Lett.*, vol. 22, no. 7, pp. 382–383, 1976.
- [7] G. Cocco, B. Costa, S. Longoni, L. Michetti, L. Silvestri, D. Tibone, and F. Tosco, "COS 2 experiment in Turin: Field test on an optical cable in ducts," *IEEE Trans. Commun.*, vol. COM-26, no. 7, pp. 1028–1036, 1978.
- [8] F. M. E. Sladen, D. N. Payne, and M. J. Adams, "Measurement of profile dispersion in optical fibres: A direct technique," *Electron. Lett.*, vol. 13, no. 7, pp. 212–213.
- [9] F. Cisternino, B. Costa, M. Puleo, B. Sordo, and E. Vezzoni, "Modal dependence of chromatic dispersion in optical fibers," in *Proc. OFC'82*, Phoenix, AZ, Apr. 13–15, 1982, p. 30.
- [10] C. Lin, A. R. Tynes, A. Tomita, and P. L. Lin, "Pulse delay measurements in single mode fibers using picosecond InGaAsP injection lasers in the 1.3  $\mu\text{m}$  spectral region," in *Proc. OFC'82*, Phoenix, AZ, Apr. 13–15, 1982, p. 28.
- [11] F. Cisternino, B. Costa, A. Moncalvo, M. Puleo, and E. Vezzoni, "Effect of OH absorption peak on material dispersion of optical fibres," presented at the 8th European Conf. on Opt. Commun., Cannes, France, Sept. 21–24, 1982.



**Bruno Costa** was born in Varapodio, Italy, in 1946. He received the Ph.D. degree in physics from the University of Torino, Torino, Italy, in 1969.

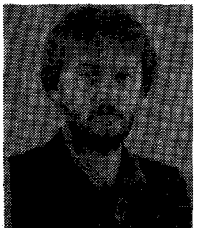
He spent one postgraduate year as an Experimental Researcher in the field of elementary particle physics. In 1971 he joined CSELT, Torino, Italy, where, after an initial period devoted to various theoretical investigations, he was engaged in research on optical fibers with special regard to the physical and transmission properties of fibers. Presently, he is Head of the Laser Section, where he is involved in activities pertaining to fiber theory, measurements, fabrication, integrated optics, and OE components study.



**Mario Puleo** was born in Borgosesia, Italy, in 1954. He received the Ph.D. degree in electronic engineering at the Politecnico di Torino, Torino, Italy, in 1978.

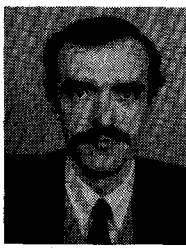
In 1979 he joined CSELT, Torino, Italy, where he is currently engaged in research on the characterization of optoelectronic devices and optical fibers.

Dr. Puleo is a member of the Italian Electrotechnical and Electronic Association.



**Daniele Mazzoni** was born in Torino, Italy, in 1956. He graduated from the Istituto Tecnico Pininfarina in 1976.

In 1977 he joined CSELT, Torino, Italy, where he is currently engaged in research on the characterization of optoelectronic devices and optical fibers.



**Emilio Vezzoni** was born in Rivarolo del Re, Italy, in 1952. He received the Ph.D. degree in electronic engineering from the University of Bologna, Bologna, Italy, in 1976.

Since 1977 he has been with CSELT, Torino, Italy, where he was engaged in the characterization of optical fibers connecting and splicing techniques. Presently, he is engaged in research on the characterization of optoelectronic devices and optical fiber propagation properties.

Dr. Vezzoni is a member of the Italian Electrotechnical and Electronic Association.

## Polarization Holding in Elliptical-Core Birefringent Fibers

SCOTT C. RASHLEIGH, MEMBER, IEEE, AND MICHAEL J. MARRONE

**Abstract**—Polarization holding in high-birefringence elliptical-core fibers is evaluated for the fiber birefringence spatial frequency range  $1.5 \text{ cm}^{-1} < \beta_i < 40 \text{ cm}^{-1}$ , corresponding to beat lengths from 1.6 mm to 4.2 cm. This range of spatial frequencies is spanned by making measurements with a broad-band light source on four fibers with different degrees of birefringence. In this way, the strength of the internal birefringence perturbations is mapped to give the first experimental measure of their power spectrum. It is shown that commonly available fiber jackets can significantly degrade the polarization holding. For low spatial frequencies, the strength of the perturbations decreases rapidly with increasing frequency, but this rate decreases by more than half over a one-and-a-half order of magnitude increase in spatial frequency. A possible origin of the perturbations is suggested and it is shown that the strength of these perturbations must be reduced if polarization holding to a very high degree is to be realized in elliptical-core fibers. Presently, internal perturbations limit the polarization holding to  $\leq 14.4 \text{ dB}$  over 1 km.

Manuscript received April 1, 1982; revised June 9, 1982. This work was supported in part by Sachs/Freeman Associates under Contract N00014-82-C-2231.

The authors are with the Naval Research Laboratory, Washington, DC 20375.

### I. INTRODUCTION

POLARIZATION holding fibers are designed to have a very large intrinsic linear birefringence  $\beta_i$  so that when light is injected into one of the linearly polarized eigenmodes it will, ideally, propagate without coupling to the orthogonal eigenmode. However, any perturbing birefringence  $\beta_p$ , resulting from either internal defects or externally-applied bends, twists, clamps, etc., whose axes are not aligned with those of  $\beta_i$  will couple the polarization eigenmodes of the fiber and degrade its polarization holding ability. For specific perturbations, for example, core ellipticity, bends, twists, and lateral pressure, for which the strength, location, orientation, and environmental dependences are known, the polarization coupling and the resulting output state of polarization can, in principle, be calculated. This becomes relatively simple if the perturbing birefringences are uniform along the fiber [1], [2]. However, in practical situations, very little is known about the origins, strengths, and distributions of these perturbations  $\beta_p$  along the fiber. Moreover, they will vary with environmental conditions